Development of radial frequency pattern perception in macaque monkeys

C. L. Rodríguez Deliz Center for Neural Science, New York University, NY, NY, USA

Gerick M. Lee Center for Neural Science, New York University, NY, NY, USA

Brittany N. Bushnell Center for Neural Science,[1] New York University, NY, NY, USA

Najib J. Majaj Center for Neural Science, New York University, NY, NY, USA

J. Anthony Movshon Center for Neural Science, New York University, NY, NY, USA

Lynne Kiorpes Center for Neural Science, New York University, NY, NY, USA

Infant primates see poorly, and most perceptual functions mature steadily beyond early infancy. Behavioral studies on human and macaque infants show that global form perception, as measured by the ability to integrate contour information into a coherent percept, improves dramatically throughout the first several years after birth. However, it is unknown when sensitivity to curvature and shape emerges in early life or how it develops. We studied the development of shape sensitivity in 18 macaques, aged 2 months to 10 years. Using radial frequency stimuli, circular targets whose radii are modulated sinusoidally, we tested monkeys' ability to radial frequency stimuli from circles as a function of the depth and frequency of sinusoidal modulation. We implemented a new four-choice oddity task and compared the resulting data with that from a traditional two-alternative forced choice task. We found that radial frequency pattern perception was measurable at the youngest age tested (2 months). Behavioral performance at all radial frequencies improved with age. Performance was better for higher radial frequencies, suggesting the developing visual system prioritizes processing of fine visual details that are ecologically relevant. By using two complementary methods, we were able to capture a comprehensive developmental trajectory for shape perception.

Introduction

Much research has been undertaken over the last 50 years to address the questions of what human infants can see and when vision matures to adult levels. Although newborns can resolve and discriminate simple contrasting patterns that are matched for total area, luminance, number of elements and contour lengths (Fantz, 1963, Fantz, 1964; Hershenson, 1964), their ability to resolve fine detail is very poor (Teller, 1981). Over the succeeding weeks, months, and years, fine spatial resolution and many other aspects of form vision become fully developed. Importantly, distinct features of visual function emerge at different ages, and thereafter they improve at different rates throughout early infancy and childhood (see Teller & Movshon, 1986; Teller, 1997; Johnson, 2011; Kovacs, Kozma, Feher, & Benedek, 1999; Braddick & Atkinson, 2011; Atkinson & Braddick, 2020, for reviews). Perceiving a visual object is a hierarchical process that builds on the processing of local cues such as oriented edges, angles, and curves. By integrating information at different spatial scales and levels of complexity, the brain can generate coherent, global representations of form

Citation: Rodríguez Deliz, C. L., Lee, G. M., Bushnell, B. N., Majaj, N. J., Movshon, J. A., & Kiorpes, L. (2024). Development of radial frequency pattern perception in macaque monkeys. *Journal of Vision*, *24*(6):6, 1–17, https://doi.org/10.1167/jov.24.6.6.

https://doi.org/10.1167/jov.24.6.6 Received February 20, 2024; published June 6, 2024 ISSN 1534-7362

(Kimchi, 1992; Kimchi, Hadad, Behrmann, & Palmer, 2005).

Existing literature on the development of global perception in children is inconclusive. Object recognition appears to shift from being based on local, category-specific features to being more dependent on global geometric shape in toddlers aged 18 to 24 months (Smith, 2009). This developmental transition from a reliance on fragments to whole object representations may reflect the visual system's early prioritization of local details before integrating them into coherent global percepts. Some reports indicate that young infants can distinguish global forms (Gerhardstein, Kovacs, Ditre, & Feher, 2004; Nayar, Franchak, Adolph, & Kiorpes, 2015), but other work using a variety of stimuli suggests that infants' ability to integrate spatial cues in service of global form perception is poor and continues to improve well into childhood (Schwartz, Day, & Cohen, 1979; Kimchi et al., 2005; Scherf, Behrmann, Kimchi, & Luna, 2009; Hadad, Maurer, & Lewis, 2010). For example, the ability to link segments of lines across space (contour completion), is measurable by 3 months of age on tasks using Gabor patches but continues to improve well into adolescence (Kovacs, 1996; Kovacs et al., 1999; Gerhardstein et al., 2004). A study in newborns tested global structure detection by habituating the observers to alternating rows of small white and black squares, finding that vertically oriented stripes were treated as novel by the infants (Farroni, Valenza, Simion, & Umilta, 2000). By 3 to 4 months of age, infants can detect form features such as symmetry and the global configuration of dot arrays and line segments (Humphrey, Humphrey, Muir, & Dodwell, 1986; Humphrey, Muir, Dodwell, & Humphrey, 1988; Humphrey & Humphrey, 1989; Curran, Braddick, Atkinson, & Wattam-Bell, 2000; Quinn, 2000). Global form detection thresholds have been tracked across development using concentric arrays of line segments embedded in noise (Gunn et al., 2002). This study found that concentric global form detection was mature by 6 to 7 years of age. Glass patterns are a canonical global form stimulus, consisting of fields of dot pairs that can be oriented and arranged to elicit the perception of global structure (Glass, 1969; Glass & Pereź, 1973). Lewis et al. (2004) studied the development of sensitivity to the global structure present in Glass patterns in 6- to 9-year-olds and adults. They found high thresholds in their youngest subjects; detection sensitivity improved to adult levels by age 9. Palomares and Shannon (2013) investigated the development of global form perception using Glass patterns and motion coherence stimuli in typically developing children and individuals with Williams syndrome. They found that both groups showed adult-like levels of motion coherence sensitivity, but had immature levels of form coherence sensitivity, suggesting that the developmental trajectory of form perception may be delayed relative to motion perception. Behavioral performance on Glass pattern discrimination tasks improves steadily throughout the first decade of life (Lewis et al., 2004). Another example of global form perception is the perception of illusory contours. Adults can reliably distinguish objects that are partially occluded or that are not defined by physical boundaries, but it is unclear at what age young children can reliably do so. Performance does not reach adult levels of discrimination until late childhood or adolescence (Nayar et al., 2015). The protracted developmental time course of global form perception is supported by electrophysiological studies in humans (Norcia et al., 2005; Pei, Pettet, & Norcia, 2007; Braddick & Atkinson, 2007). Visually evoked potentials specific to global form processing emerge later, but develop at a faster rate than the neural signature for global motion perception (Braddick, Atkinson, & Wattam-Bell, 2003; Palomares, Pettet, Vildavski, Hou, & Norcia, 2010; Wattam-Bell, Atkinson, & Wattam-Bell, 2010; Braddick & Atkinson, 2011).

A big limitation of human studies is that longitudinal data are rarely available and typically focus on one or a few selected ages, leaving large age gaps and providing us with only snapshots of performance at particular points in developmental time. Moreover, only limited amounts of data can be obtained from a given subject in most cases. These limitations can be overcome by studying animal models. Macaque monkeys are particularly well-suited for this work because the monkey visual system is highly similar to that of humans, but visual performance develops roughly four times faster than humans, making it possible to track changes in visual behavior throughout development (Teller & Movshon, 1986; Teller, 1997). The development of the macaque visual system has been extensively characterized by our laboratory and others, both at a behavioral and neurophysiological level (see Boothe, Dobson, & Teller, 1985; Blakemore & Vital-Durand, 1986; Kiorpes & Kiper, 1996; Teller, 1997; Chino, Smith, Hatta, & Cheng, 1997; Kiorpes & Movshon, 2004; Daw, 2006; Kiorpes & Movshon, 2014; Danka Mohammed & Khalil, 2020).

Prior studies of the development of global form perception in monkeys, as measured using oriented Gabor patches in a contour integration task and Glass patterns, showed that sensitivity is measurable around 16 weeks. These abilities continue to improve into the second year of postnatal life (Kiorpes & Bassin, 2003; Kiorpes, Price, Hall-Haro, & Movshon, 2012). Perception of simple textures, however, is already evident by 6 weeks of age, and matures relatively early (El-Shamayleh, Movshon, & Kiorpes, 2010). The common denominator shared by all of these types of global form stimuli is the underlying requirement of detecting and integrating local contrast, orientation and spatial frequency cues across space while discriminating fine details in the image (Wilson, Wilkinson, & Asaad,

1997; Wilkinson, Wilson, & Habak, 1998; Badcock, Clifford, & Khuu, 2005; Wang & Hess, 2005; Badcock & Clifford, 2006; Poirier & Wilson, 2006).

In this work, we assessed infant macaques' sensitivity to radial deformation of circular contours using radial frequency (RF) stimuli (Wilkinson et al., 1998). RF patterns are a useful stimulus class to assess global shape processing because these patterns represent a wide array of smooth closed shapes that are commonly seen in nature, like fruits and flowers (Wilkinson et al., 1998; Hess, Achtman, & Wang, 2001; Hess, Wang, & Dakin, 1999; Jeffrey, Wang, & Birch, 2002; Loffler, Wilson, & Wilkinson, 2003). Perception of these patterns requires integration of information across space to accurately perceive the overall shape of the stimulus. Evidence shows that even though the circular contour is continuous, detecting deformations from circularity relies on comparing orientation information at different points along the contour rather than depending on local cues at a single point (Wilkinson et al., 1998; Hess et al., 1999; Loffler et al., 2003; Jeffrey et al., 2002). Adults show remarkably high sensitivity to RF patterns, with thresholds reaching hyperacuity levels (Wilkinson et al., 1998). In other words, adult observers are able to resolve spatial distinctions at a scale finer than simple spatial resolution (Westheimer, 2010). Previous hyperacuity studies in infant humans and monkeys using traditional Vernier stimuli showed a protracted developmental time course for this ability as compared with grating acuity (Manny & Klein, 1984; Shimojo, Birch, Gwiazda, & Held, 1984; Shimojo & Held, 1987; Norcia, Manny, & Wesemann, 1988; Kiorpes, 1992; Zanker, Mohn, Weber, Zeitler-Driess, & Fahle, 1992; Brown, 1997; Carkeet, Levi, & Manny, 1997; Skoczenski & Norcia, 2002; Wang, Morale, Cousins, & Birch, 2009; Kiorpes, 2015), suggesting that RF discrimination might also show protracted development. One previous study of young human infants showed that they displayed poor sensitivity to RF patterns, with a period of rapid maturation between 4 and 6 months of age, followed by an extended period of slower improvement (Birch, Swanson, & Wang, 2000). The developmental trajectory of sensitivity to radial deformations in macaques has not yet been studied. We tested macaque monkeys (aged 2 months to 10 years) on RF discrimination tasks. We describe the development of global form sensitivity within and across subjects, demonstrating that even the youngest monkeys in our cohort could discriminate between RF patterns and circles, but their behavioral sensitivity continued to improve well beyond the first year of life. We found it expedient to use a novel four-choice oddity task to track performance in younger animals, which complemented data obtained using traditional forced-choice methods such reinforced looking and bar pulling, depending on the subject's age. This combined approach allowed us to capture the full developmental trajectory of RF sensitivity using a consistent task. We show that both tasks reliably capture the developmental trajectory of global form perception, with a predictable difference in sensitivity between tasks. Overall, our data reflect a developmental improvement in the perception of global shape information that is contingent on the spatial extent over which the visual system is able to integrate signals.

Methods

Subjects

Eighteen visually normal pig-tailed macaque monkeys (*Macaca nemestrina*) participated in this study—4 females, 14 males. At the time of testing, their ages ranged from 8 to 491 weeks. Twelve subjects were tested at multiple age points throughout development and six were tested cross-sectionally. Subject-specific details are presented in Table 1. All animal care and experimental procedures were approved by the Institutional Animal Care and Use Committee of New York University and were in compliance with the guidelines established in the National Institutes of Health Guide for the Care and Use of Laboratory Animals.

Visual stimulus display

Stimuli were generated using custom software developed in our lab. The display consisted of a gamma-calibrated CRT monitor, placed at a distance determined by each behavioral setup.

For the two-alternative forced choice (2-AFC) experiments, stimuli were presented on a monitor with a resolution of 1,024 × 768 at 100 Hz and a mean luminance of 30 cd/m^2. The screen subtended 43.6° at a viewing distance of 50 cm and pixel size was 0.043° in the reinforced-looking paradigm. Older animals tested on a 2-AFC bar-pulling paradigm worked at a viewing distance of 100 cm, where the screen subtended 22.6° and pixel size was 0.022°. The display for the four-choice experiments was a monitor with a resolution of 1,280 × 960 at 120 Hz and a mean luminance of 28 cd/m^2, combined with an EyeLink 1000 (SR Research, Kanata, Ontario, Canada) eye tracker. Viewing distance was 114 cm, at which the monitor subtended 20° × 15° and pixel size was 0.016°. Stimulus size was equated across the different viewing set ups, independent of pixel size.

RF stimuli

To characterize the development of global form sensitivity, we used RF stimuli (Figure 1A), a family of circular contours in which the cross-section of

Subject	Ages tested (weeks)	Task	Bino/Mono	Lens (R/L)
M1 (female)	16, 20, 60, 80, 88, 92	4-choice	BINO	–/–
M2 (female)	16, 20, 56, 84, 88	4-choice	BINO	–/–
M3	12, 16, 28, 32, 52	4-choice	BINO	–/–
M4 (female)	28, 32	4-choice	BINO	–/–
M5	16, 24, 28, 32, 48, 60	4-choice	BINO	–/–
M18	8, 12, 24, 32	4-choice	BINO	–/–
M6	68, 180**	Both	BINO	–/–
M7	67, 180**	Both	BINO	–/–
M8 (female)	20*, 77, 181	2-AFC	BINO	–/–
M9	17*, 73, 173	2-AFC	BINO	–/–
M10	30	2-AFC	BINO	–/–
M11	52, 158	2-AFC	BINO	–/–
M12	48, 135, 199, 230	2-AFC	MONO	+1.0 D /+1.0 D
M13	353	2-AFC	MONO	–/+1.75 D
M14	125, 237	2-AFC	BINO	–/–
M15	99	2-AFC	BINO	–/–
M16	491	2-AFC	MONO	+2.0 D/+2.25 D
M17	433	2-AFC	MONO	+1.25 D/+1.0 D

Table 1. Behavioral subjects *2-AFC*, two-alternative forced choice.

Note: Identification, ages at which at least one radial frequency type was tested, task modality are listed in the first three columns. The last two columns indicate whether the subject was tested with both eyes (BINO) or one eye at a time (MONO), and whether they were tested using a corrective lens (R/L). Only data from the dominant eye was included for these subjects. M1–M7 are the same as M1–M7 in (Lee et al., 2024).

*Ages tested with the reinforced looking paradigm.

**Ages tested with the four-choice oddity task for subjects that were also tested on the 2-AFC task.

the outline's luminance profile is determined by a fourth-derivative Gaussian. These were designed by Wilkinson et al. (1998) with the goal of defining shape space parametrically to measure shape selectivity and sensitivity in psychophysical experiments. The control–distractor–stimulus in our study is the base circle. Unique stimuli can be generated from the base circle by sinusoidally modulating the contour a given number of times to create different shapes. The amplitudes of these modulations can be parametrically adjusted so that the stimulus is either like the base circle or not (Figure 1B). For our study, we kept the stimulus radius fixed at 1.5° and the carrier spatial frequency at 2 cycles per degree. This spatial frequency ensures our stimuli were within the range of peak contrast sensitivities for our youngest subjects (Boothe, Kiorpes, Williams, & Teller, 1988), while still being suitable to characterize performance at older ages (Wilkinson et al., 1998).

Psychophysical experiments

Four-choice oddity task

We designed a new four-choice oddity discrimination task that implements high-speed eye tracking (EyeLink 1000, SR Research), task automation (MWorks) and reward systems to decrease the time needed for training and testing subjects. This method allowed us to assess sensitivity to RF stimuli across development starting at young ages, with an automated procedure, while maximizing the number of trials a subject completes in each session. Before testing, we trained five infant monkeys to sit in a custom-designed testing chair and fixate on a screen, head-free, starting at approximately 6 postnatal weeks. Two juveniles that had previously been tested using 2-AFC (described elsewhere in this article) were also trained to perform the four-choice oddity discrimination task. A total of eight subjects were tested on this paradigm.

A trial began with a gray screen and a 1° to 2° red, central fixation square. A trial was initiated when the subject fixated on the center of the screen, which triggered the disappearance of the fixation square, followed by a 200 ms delay and the subsequent presentation of a 2 × 2 array of stimuli of equal size (3°) centered at ±3.2° in both directions such that each stimulus was approximately 4.5° eccentric from the center of the screen (Figure 1C). Three of the stimuli were distractors (circles) and one was the target, a modulated RF stimulus. Subjects were required to

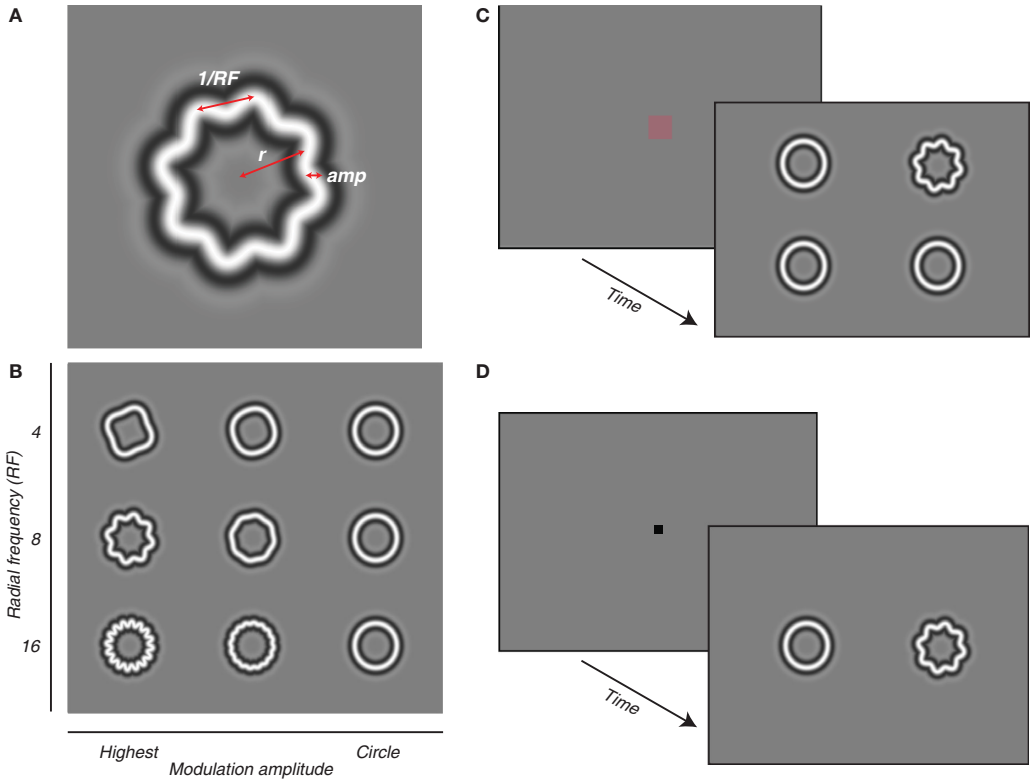

Figure 1. Radial frequency (RF) stimuli and task diagrams. (**A**) Each stimulus is defined by a RF, amplitude (amp), and size (mean radius, r). (**B**) We used the three RF types (4, 8, and 16), shown on the ordinate. Modulation amplitude is plotted along the abscissa, depicting a sample of modulations that are increasingly harder to discriminate from the base circle. (**C**) On each trial of the four-choice oddity task, subjects were required to fixate on the central fixation point. Four stimuli then appeared on the screen, equidistant from the center. Three stimuli were distractor circles, the target was a RF pattern of varying amplitude modulation. Subjects are required to identify and fixate on the target for 400 ms. (**D**) On each trial of the 2-AFC task, two stimuli appear on the screen, one is a distractor circle and the target is a RF pattern. Subjects are required to indicate the side on which the RF pattern appeared.

saccade toward the target and maintain fixation on it for 400 ms within a 5° window for the trial to be considered a hit and rewarded with age-appropriate liquids. A small proportion (approximately 5%) of catch trials were included to assess for any positional bias. To ensure accurate classification of trials, we extracted saccade and eye position data from MWorks output files. With this, we classified trials based on eye position and the subject's behavior. Correct trials were any trial during which the animal fixated on the target for the full 400 ms. Failed trials were parsed into two categories: a miss if the animal fixated a distractor and ignored/no decision trials, in which the animal did not fixate any location for the full 400 ms. Ignored trials were excluded from our analysis. We randomly chose difficulty on a trial-to-trial basis, using the method of constant stimuli. To encourage cooperative behavior, it was our standard procedure to allow a larger amount of easy trials throughout the session. To characterize their perceptual thresholds, data were collected using a method of constant stimuli with a range of octave-spaced modulation amplitudes for a three RF types (4, 8, and 16).

Two-AFC task

We used standard operant conditioning methods to test visual performance in as previously described (Boothe et al., 1988; Kiorpes & Movshon, 1989; Kiorpes, Kiper, & Movshon, 1993; Kozma & Kiorpes, 2003; El-Shamayleh et al., 2010). Fourteen monkeys were trained to perform an operant two-alternative forced-choice discrimination task. At the time of testing, their ages ranged from 17 to 491 weeks, allowing us to track development of form sensitivity over the long term. Infants were allowed to roam freely in a cage equipped with a face mask. Photocells embedded in the mask signaled when they placed their faces in the mask and triggered a new trial.

Stimuli appeared 5° from the center on either side of the central fixation point. The stimulus was present on the screen for a minimum of 500 ms and a maximum

of 3,000 ms before the trial ended. The animals were shown a modulated RF stimulus on one side and a circle on the other. Animals were trained on a reinforced looking paradigm (Kiorpes & Kiper, 1996), generating a saccade to the target (for macaques younger than 20 weeks) or pulling a bar to indicate whether the target stimulus was located on the left or the right side of the screen (Figure 1D). Monkeys received a small juice reward for correct trials and an error tone followed by a short pause if incorrect.

The goal was to find a range of five modulation amplitudes spanning the subject's perceptual threshold from near perfect (100%) to near chance (25% on the four-choice oddity and 50% on the 2-AFC). Difficulty was increased by parametrically decreasing the modulation amplitude of the pattern, making it harder for the subject to discriminate between circles and RF stimuli. Once threshold values were identified, we then counterbalanced by collecting a final session per RF type in the reverse order as they were initially presented, to control for testing and order effects.

Data analyses

Wilkinson et al. (1998) reported that, for human observers, sensitivities were typically better for higher radial frequencies, which may reflect differences in curvature-processing mechanisms across RF types. Therefore, we measured modulation thresholds separately for each RF type. Sessions collected within the same 7-day span were combined for a given age point.

Threshold estimation

For the 2-AFC task, thresholds were estimated based on 75 trials per stimulus condition. Threshold values for this task were obtained by using a probit regression to determine the interpolated value corresponding to 75% correct performance. To compare the developmental trajectories derived from our oddity task and data collected using our standard 2-AFC task (e.g., Kiorpes, Price, Hall-Haro, & Movshon, 2012), we matched our four-choice threshold distributions by identifying the performance criteria that corresponds to 75% correct performance on a 2-AFC task, at which $d' = 0.95$ (Hacker & Ratcliff, 1979).

Thresholds for the four-choice oddity task were estimated on a minimum of 100 trials per stimulus condition to ensure robust definition of slope and threshold values. We fit a cumulative of the Weibull distribution to the performance data to estimate the behavioral threshold (Wichmann & Hill, 2001a). We used a maximum likelihood fitting process to extract a shared slope and lapse parameter, and a separate threshold for each individual measurement. Thresholds were computed as the intercept of the Weibull at 53.7% correct, corresponding to a d' of 0.95. We estimated variability using a parametric bootstrap by fixing slope and lapse rates to the values extracted from the original fitting routine (Wichmann & Hill, 2001b).

Sensitivity measurements

Developmental trends for all tasks were defined by fitting a Michaelis-Menten function to fitted sensitivity (1/threshold) data as a function of age using the equation:

$$S = S_{\max}\left[\frac{A}{A+C}\right], \quad (1)$$

where S is the fit sensitivity, S_{max} is the peak sensitivity, A is the subjects' age in weeks, and C is the criterion age at which sensitivity reached half its maximum value (semisaturation point). S_{max}, A, and C are free parameters, estimated from the fits computed by minimizing the squared error of the model predictions. The half-maximum age C provides an indicator of the rate of development, with lower values suggesting a faster rate, because half-maximum sensitivity is reached at a younger age. Fits were computed by minimizing the squared error of the model predictions. The data were bootstrapped 1,000 times by resampling data for each RF with replacement to extract parameter C (half-maximum age) on each iteration and compute 95% confidence intervals. Comparing the half-maximum ages across different conditions allows us to infer relative rates of sensitivity development.

Results

Measuring RF sensitivity

For each of our animals, we measured perceptual thresholds for RF stimuli in a series of four-choice oddity and/or 2-AFC experiments. Data were collected with a combination of longitudinal and cross-sectional testing. We used a block design to test each RF (RF4, RF8, or RF16) separately. We examined performance on catch trials, in which all stimuli were identical, to evaluate potential biases toward particular screen locations. No systematic positional response biases were evident across subjects based on catch trial accuracy.

Figure 2 shows example psychometric curves measured for two infant macaques tested on the four-choice task at 16 weeks of age. Performance at a given age varied across the radial frequencies tested, as shown by the horizontal separation between the red (RF4), blue (RF8), and green (RF16) curves. For all three radial frequencies tested, our new four-choice

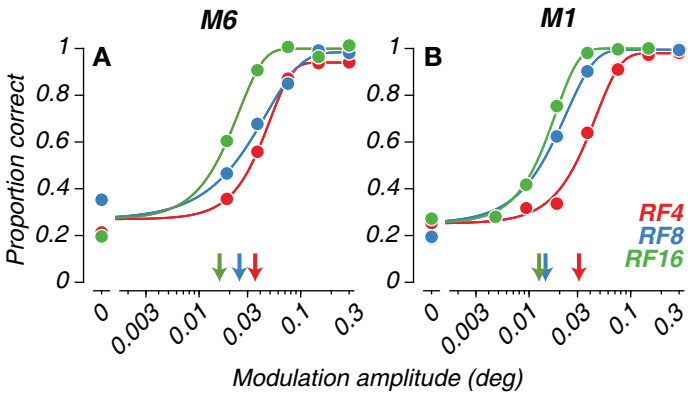

Figure 2. Example four-choice data from two 16-week-old macaques. (**A** and **B**) Psychometric curves computed for infant macaques tested on each of three radial frequencies. Mean performance (solid circles) for each modulation amplitude level was fit with a Weibull. Radial frequency type is indicated by color (red = RF4; blue = RF8; green = RF16). Isolated points along the ordinate indicate performance on catch trials. Arrows indicate threshold amplitudes.

oddity task yielded lawful psychometric functions. In both cases, sensitivity to modulation for the highest RF was better. We took the threshold for each function to be the amplitude supporting 53.7% correct performance in this task (indicated by arrows).

We tested a total of 18 animals, 13 at more than one age. Two (M6 and M7) were tested on both paradigms at different ages. However, these subjects were tested at substantially different ages using the two methods: M6 at 68 weeks on the four-choice task and 180 weeks on the 2-AFC task; M7 at 67 weeks on the four-choice task and 180 weeks on the 2-AFC task. Given the significant age difference between the testing sessions and the differences in sensitivity captured by the two tasks, it is difficult to make meaningful comparisons of their individual modulation sensitivities across the two methods. Therefore, we focused our analysis on the overall trends observed across the larger sample of subjects tested on each task, rather than drawing conclusions from the limited data available from these two subjects. Figure 3 shows the RF discrimination performance as sensitivity (inverse of threshold) to modulation amplitude, as a function of RF for those 13 animals. Test age in weeks is indicated next to each dataset. In most cases, sensitivity improved with age. However, the data also reveal some individual variability in developmental trajectories across subjects. In some cases, like Figures 3B–3D, for example, the animal's motivation may have fluctuated over sessions and age, resulting in lower estimated sensitivities than one would expect given the animal's earlier performances. Overall, the developing improvement in modulation sensitivity is clear in spite of some variability, possibly reflecting maturation of neural mechanisms for RF processing. Moreover, the pattern of higher modulation sensitivity for higher RFs was evident across most subjects, and for each task modality.

Developmental time course of RF sensitivity

To look for overall trends across all subjects and methods, longitudinal and cross-sectional data for all subjects is shown in Figure 4. The inclusion of cross-sectionally tested subjects confirms we are capturing developmental improvements rather than training effects alone, as these subjects' sensitivities fall within the trajectory delineated by the longitudinal data. Our 2-AFC data (Figures 4D–4F) showed clear developmental asymptotes for all RFs, likely due to more data from older subjects. Meanwhile, the four-choice data (Figures 4A–4C) had most clearly begun to asymptote for the highest radial frequencies at the older end of the age range we tested. Another interesting feature of our data is the magnitude of sensitivities computed using reinforced looking at the earliest ages tested on the 2-AFC task (cross symbols; Figures 4D–4F). These variations likely reflect the impact of temperament and engagement of the very young subjects on the difficult range of modulation amplitudes the experimenter could effectively test, yielding lower estimates of sensitivity. These data points are included in Figures 4D to 4F for completeness in visualizing our data across all subjects, but we exclude them in the analysis described below for reasons that are explained elsewhere in this article.

To determine whether there was a difference between the developmental trajectories as measured with the four-choice oddity task and traditional 2-AFC bar-pulling methods, we took account of the fact that discrimination experiments with more than one alternative increase the number of distributions of a decision variable (Kaplan, Macmillan, & Creelman, 1978). Therefore, the distributions onto which the decision variable is mapped in a 2-AFC task are not equal to those implemented by the observer on a four-choice task and performance estimates cannot be directly compared across variable-alternative paradigms. We extracted four-choice performance estimates based on a 53.7% threshold to match our 2-AFC performance. We then fit Michaelis–Menten functions to the developmental trends across both populations simultaneously and for each individual subject using a constant offset fitting routine, with the semisaturation point constrained across the two data sets $N_{2\text{-}AFC} = 10$, $N_{4-choice} = 6$, and $N_{both} = 2$. In other words, we fit the data from both tasks jointly, allowing for a constant offset to account for potential systematic differences in threshold for the two methods. We excluded the reinforced looking

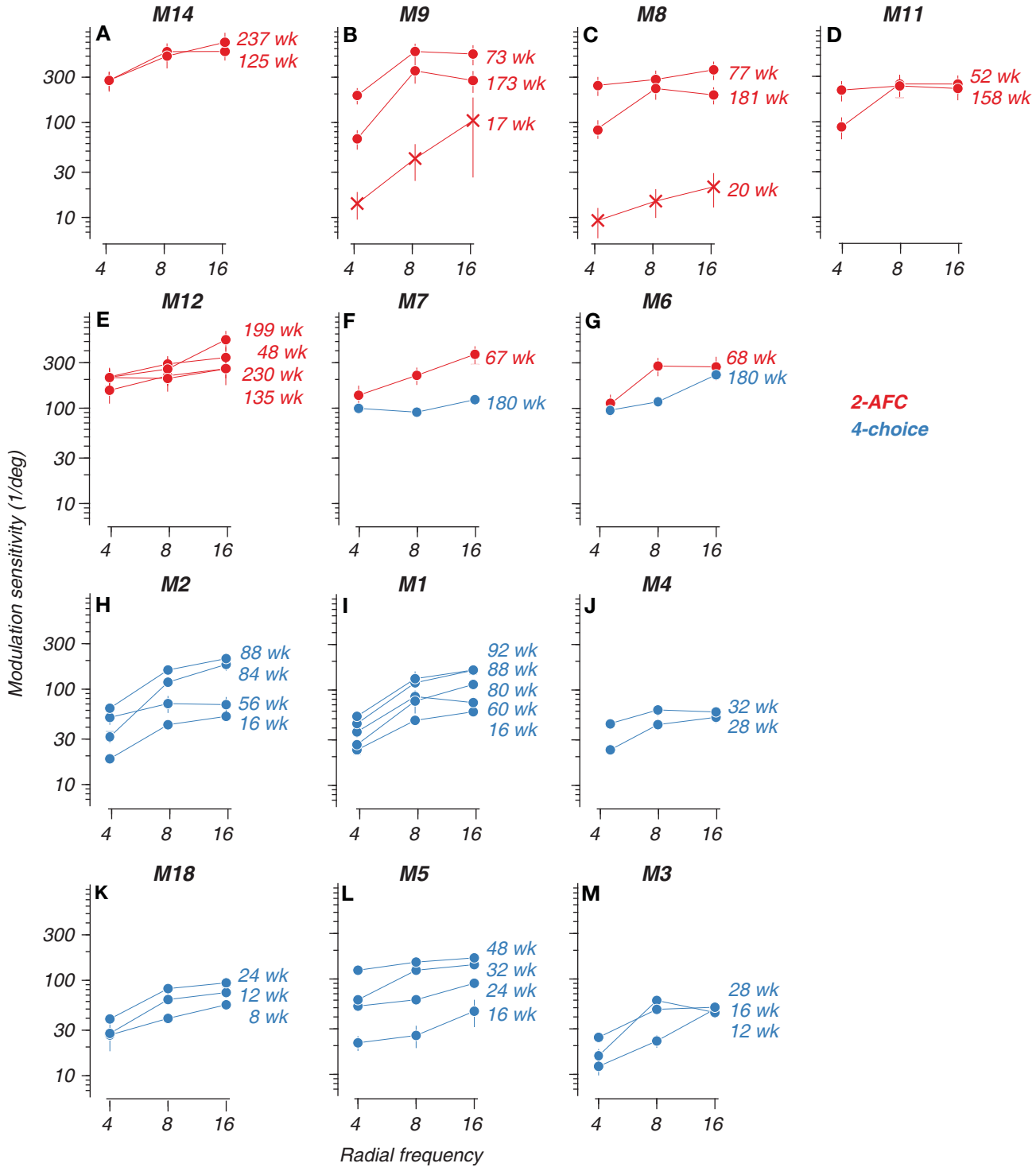

Figure 3. Development of sensitivity to radial frequency stimuli. (**A**–**M**) Perceptual sensitivity of all subjects tested at more than one age. Sensitivity to modulation amplitude (inverse of threshold) as a function of radial frequency. Cross symbols in (**B**) and (**C**) correspond with reinforced-looking data. Red = 2-AFC and blue = four-choice data. The age in weeks of the subject at the time of testing is indicated next to each curve. Error bars represent 68% confidence intervals.

data from the 2-AFC–derived set for this analysis because of the sparse number of data points collected, and this testing method may differ from either the 2-AFC and four-choice tasks in ways that require further examination. Exclusion of the reinforced looking data combined with the joint fitting method allowed for more reliable estimates of the rate and extent of development. Our results show that global

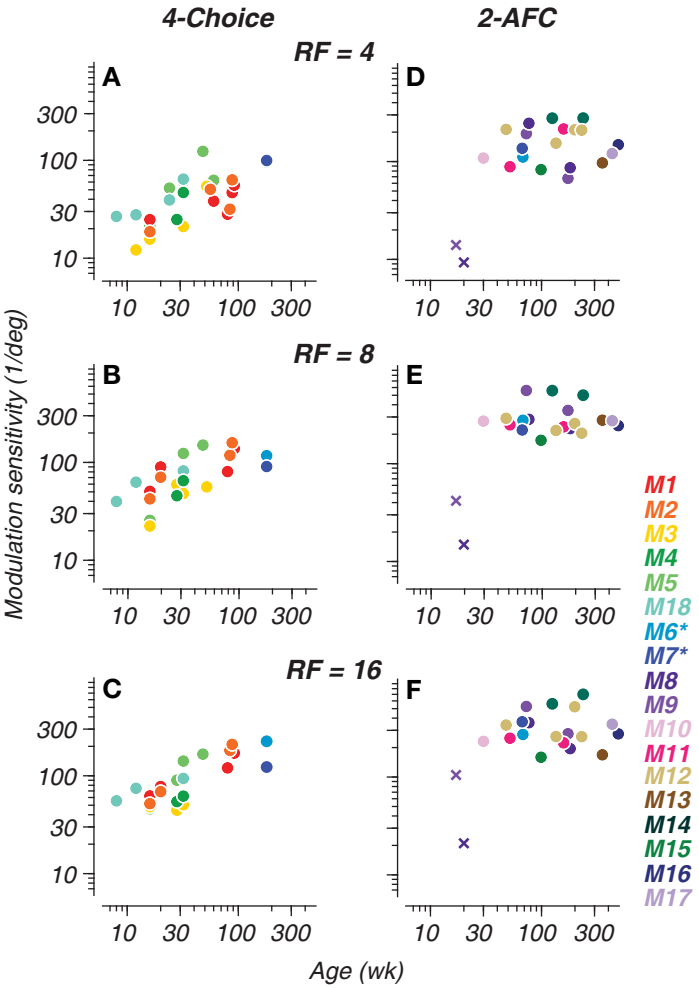

Figure 4. Tracking radial frequency (RF) sensitivity development with a four-choice oddity task and a two-alternative forced choice (2-AFC) task. Modulation sensitivity for all subjects plotted as a function of age in weeks. (**A–C**) Data collected with the four-choice oddity task. (**D–F**) Data collected with the 2-AFC task. Subject identity is indicated by symbol color. Cross symbols represent reinforced-looking data. Asterisks on legend indicate that monkeys 6 and 7 were tested on both tasks. Subjects M10, M13, and M15–M17 were only tested once using the 2-AFC task.

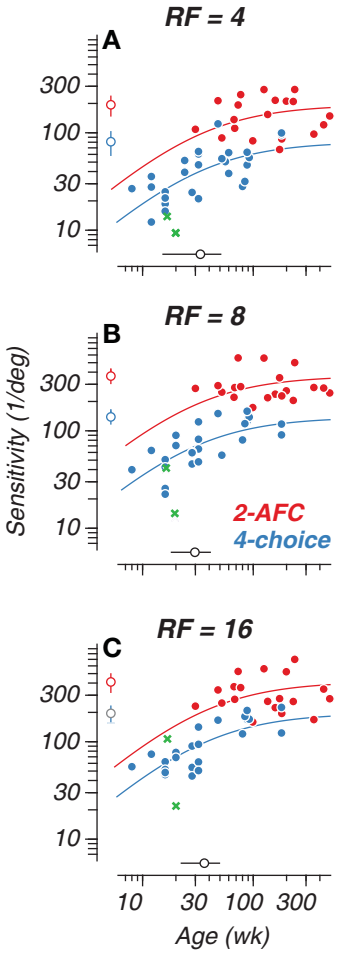

Figure 5. Jointlyfit 2-AFC and 4-choice sensitivity data. Panels **A–C** depict grouped 2-AFC and 4-choice data that were jointly fit with a constant sensitivity offset. The smooth curves represent Michaelis-Menten fits to the data across subjects for each task. The isolated open symbol intersected by vertical bars located alongside the ordinate represents the peak sensitivity value for each curve; the open symbol intersected by horizontal bars on the abscissa represents the semi-saturation age. Error bars represent ±1 SD. Green cross symbols correspond to reinforced-looking data, excluded from fitting.

form perception was present by the earliest ages we tested (8–10 weeks), improved gradually, and was superior for high radial frequencies. Our results, plotted in Figures 5A to 5C, show that both tasks reliably capture a similar developmental trajectory for RF pattern perception, with an approximately two-fold scaling difference between tasks. Peak sensitivity is represented by open circles and the fixed half-maximum age is represented by the open black symbol along the abscissa with horizontal/vertical bars indicating ±1 standard deviation of the fit. Our data suggest that both types of psychophysical tasks can yield reliable performance characterizations longitudinally and cross-sectionally throughout development. Moreover, our complementary tasks provide enhanced characterization of global form perception, capturing the full developmental picture.

Trends for the semisaturation point and peak sensitivity across RF types are plotted in Figures 6A and 6B. Vertical bars indicate ±1 standard deviation of the fit. Estimated peak sensitivity was lower overall for the four-choice oddity task at 80.95 ±23.14, 138.8 ±23.07, and 195.5 ±40 deg^{-1} for RF4, RF8, and RF16, respectively. On the 2-AFC task, sensitivities peaked at 193.7 ± 47.08, 364.4 ± 63.00, and 410.6 ± 94.05 deg^{-1} for RF4, RF8, and RF16, respectively. The constant sensitivity offset used in the joint fitting

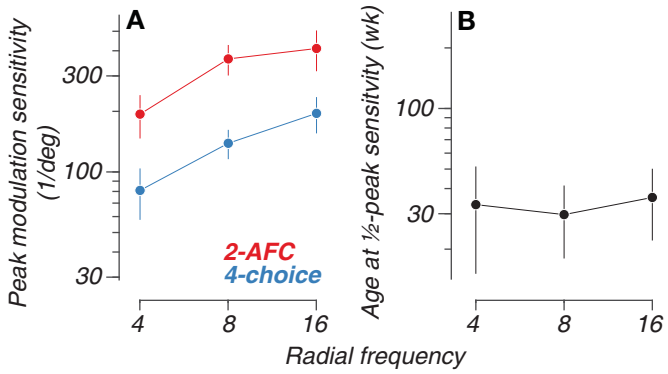

Figure 6. The rate and extent of the development of radial frequency sensitivity. (**A**) Estimated peak sensitivity for both paradigms. (**B**) Estimated joint half-maximum age values for each radial frequency type. Error bars indicate ±1 standard deviation. Animals plotted in red were tested on two-alternative forced choice, whereas animals plotted in blue were tested on the four-choice task.

of the 2-AFC and four-choice data can be determined from the proportion between the peak sensitivities of the two curve fits. The offset between the 2-AFC and four-choice peak sensitivity values is 2.39, 2.62, and 2.10 for RF4, RF8, and RF16, respectively. These differences represent the constant vertical shift allowed between the two curves during the fitting process, accounting for the systematic differences in sensitivity between the two tasks while estimating a common developmental trajectory. We also found that sensitivity reached semisaturation at 33.29 ± 18.21, 29.70 ± 11.72, and 36.14 ± 14.05 weeks of age for RF4, RF8, and RF16, respectively, when accounting for both task modalities. Similar measures computed for contour integration and linear Glass patterns show half-maximum ages of 37 and 47 weeks, respectively (Kiorpes & Bassin, 2003; Kiorpes, Price, Hall-Haro, & Movshon, 2012). The consistency between the semisaturation point calculated here for RF patterns (approximately 30–36 weeks) and those from previous findings helps to validate our RF methodology and captures development as being on a similar time course as established with other global form stimuli.

We found that modulation sensitivity matures at similar rates for all three RFs tested. However, on both 2-AFC and four-choice tasks, RF4 exhibits a significantly lower peak sensitivity compared with RF8 and RF16 ($p < 0.05$; bootstrap hypothesis test). Modulation sensitivity for RF8 peaks lower than that for RF16, but this is not statistically significant. Despite overlap in the developmental trajectories, the observed differences in peak modulation sensitivity between low and high RFs raise the possibility for possible divergence in the form mechanisms that are selectively responsive to coarse or fine visual features.

Discussion

In this study, we sought to characterize the developmental trajectory of infant macaques' intermediate-level shape perception. We tested animals on a RF pattern discrimination task in which they were required to discriminate between closed contours with radii modulated by a sinusoidal function of polar angle and contours with no modulation (circles). We used a range of radial frequencies (4, 8, and 16) and five to six modulation amplitudes for each to vary the difficulty of this discrimination. Our results suggest that perception of global form continues to develop well beyond the first year of life. Human studies show that sensitivity to RF stimuli matures rapidly during the first year of life, but continues to improve into early childhood (Birch et al., 2000).

Our infant monkeys could discriminate all radial frequencies tested as early as 8 to 10 weeks postnatal, as shown using an automated four-choice oddity task. Sensitivity for all radial frequencies improved with age, with an overall trend of higher sensitivity for higher radial frequencies. These developmental trends are also captured with separate measurements using a 2-AFC discrimination task. When compared directly, data from the two tasks improved in parallel, with a roughly two times scaling difference between sensitivity measures using equated performance metrics. The inclusion of the 2-AFC task, which has been widely used in previous studies of visual development, serves to validate our novel four-choice oddity task as a reliable method for assessing RF sensitivity across a broad range of ages. The four-choice oddity task can now be applied to investigate the development of a wide range of visual functions, providing a valuable tool for future studies of visual development in macaques.

Time course of global form development

Circles have a constant curvature along their contour, whereas RF stimuli are created by systematically varying the frequency and degree of modulation amplitude. The visual system's job is then to measure the variability of the curvature responses between both kinds of patterns, a computation that is not available to local curvature discrimination mechanisms (Wilkinson et al., 1998; Poirier & Wilson, 2006; Bell, Badcock, Wilson, & Wilkinson, 2007; Loffler, 2008). Our findings build on and expand prior research on the development of global form perception in infant humans and monkeys. Although informative, past human work was limited by sparse longitudinal data and restricted age ranges. The current study helps to address these limitations through a mixture of longitudinal and cross-sectional testing of infant macaques from

2 months to 10 years and the implementation of a novel four-choice oddity task, allowing for the characterization of global form perception across development. Our approach is more feasible in macaque studies compared with human studies, where it is challenging to retain participants over extended periods. Although not explicitly included in our results, the growth curves for subjects tested at four to five age points with the four-choice task (e.g., M1–M3) can be fit independently and yield similar results to the group growth curves. This strategy allows us to estimate peak sensitivities and half-maximum ages that describe the average developmental trajectory of this perceptual function from data collected across multiple subjects at different age points. Although the current study did not compare individual growth curves directly with the group curve, our experimental design provides the opportunity for such analyses in future work. However, the variability in the number of data points per subject and the specific ages tested across subjects may limit the extent to which detailed comparisons can be made. Nonetheless, our data lay the foundation for exploring the individual differences in the development of RF sensitivity, which could provide valuable insights into the factors influencing the maturation of this perceptual ability.

By fitting our data with a Michaelis–Menten function to characterize the relationship between sensitivity and age, we are, in effect, measuring the rate of maturation. The Michaelis–Menten function is a saturation rate function and has a similar shape to that commonly observed in developmental data: a rapid initial increase followed by a plateau. Trying to describe the speed of sensitivity development may not be an easily or intuitively interpretable metric, so instead we interpret the half-maximum ages as an indicator of the rate at which maximum sensitivity is reached for each condition studied. The rate of improvement of global form perception in our study was faster initially and then slowed down over the first three years of age in primates, roughly corresponding to the first 10 years of human childhood, consistent with human research on RF pattern perception (Birch et al., 2000; Wang et al., 2009). Moreover, our findings are consistent with studies on other types of global form perception, such as contour integration and Glass pattern discrimination, which depend on spatial integration across the large regions of an image and also show protracted developmental timelines (Kiorpes & Bassin, 2003; Kiorpes & Movshon, 2003, Kiorpes & Movshon, 2004).

Local versus global processing

Previous studies using RF stimuli have noted that thresholds are in the hyperacuity range (Wilkinson et al., 1998). Adult macaque data also reach the hyperacuity range. The extended developmental trajectory for RF discrimination is consistent with hyperacuity development in macaques reported by Kiorpes (1992); (Kiorpes 2015) on the development of grating and Vernier acuity in macaques. In that study, grating acuity was relatively more mature in early postnatal life than Vernier acuity, with Vernier acuity maturing at a faster rate over a longer time course. Wilkinson et al. (1998) studied the relationship between RF and perceptual thresholds, finding that radial frequencies below 2 resulted in drastically higher thresholds. Radial frequencies of 3 to 24, including the range used in the present study, led to thresholds that plateaued between 2 and 9 seconds of arc.

These values fall well below the cutoff for hyperacuity (Hess et al., 1999; Jeffrey et al., 2002; Wang & Hess, 2005; Schmidtmann & Kingdom, 2017). The increasing peak sensitivities for higher RF types observed across our subjects may, therefore, be due to increased information necessary for the observer to resolve spatial distinctions at scales that exceed the layout of receptors tiling the retina. Our study may also provide support for the use of RF stimuli as a resource to test hyperacuity in the diagnostic process for amblyopia in children (Subramanian, Morale, Wang, & Birch, 2012).

Recent work by Baldwin, Schmidtmann, Kingdom, and Hess, (2016) and Schmidtmann and Kingdom (2017) suggests that local curvature cues alone may be sufficient for the detection and discrimination of RF patterns. These findings challenge the notion that global integration across the entire stimulus is necessarily required for processing all RFs. The model proposed by Poirier and Wilson (2006) also supports the idea that curvature mechanisms could mediate RF perception without relying on global pooling. However, there is substantial evidence indicating that spatial integration plays a key role in this perceptual function. Wilkinson et al. (1998) showed that thresholds increased for lines compared with closed contours, suggesting that the continuity of the contour is important. Hess et al. (1999) demonstrated that disrupting the contour continuity of RF patterns impairs performance, even for smoothly modulated patterns. Loffler et al. (2003) also found that interfering with the closed nature of the contour led to increased thresholds. The relative contributions of local and global cues likely depend on the specific RF. Jeffrey et al. (2002) provided a local analysis predicting that thresholds would continue to improve with increasing RF due to greater local orientation and curvature changes. They found that radial deformation thresholds depended primarily on the circular contour frequency (cycles of modulation per degree of unmodulated contour) rather than the absolute RF. At a given radius, higher RF patterns have greater circular contour frequency.

For example, at a radius of 1.5°: RF4 has a circular contour frequency of 0.43 cycles/degree, RF8 has 0.86 cycles/degree, and RF16 has 1.72 cycles/degree. Jeffrey et al. (2002) showed thresholds improve linearly with log circular contour frequency until reaching a plateau around 1.3 to 2.6 cycles/degree. The lower peak sensitivity we observed for RF4 is likely because a circular contour frequency of 0.43 cycles/degree is well below the plateau region found by Jeffrey et al., (2002), whereas RF8 and RF16 at a 1.5° radius are close to or above the plateau circular contour frequency where asymptotic sensitivity is reached. The lack of significant difference between RF8 and RF16 peak sensitivity is consistent with their thresholds both being on the plateau portion of the function. The circular contour frequency finding from Jeffrey et al. (2002) has interesting implications for the debate about whether RF pattern perception requires spatial integration across the broader stimulus by higher visual areas. On one hand, the circular contour frequency result shows that RF thresholds depend on the local spacing of modulation cycles along the contour rather than the overall stimulus size or RF number. However, the plateau in circular contour frequency tuning still extends over multiple cycles (1.3–2.6 cycles/degree), suggesting integration of local cues. Our findings of similar peak sensitivities for RF8 and RF16 are consistent with this idea of an upper limit on global integration. Regarding the dependence of radial deformation sensitivity on stimulus parameters, Wilkinson et al. (1998) tested a range of values for RF, carrier spatial frequency, mean radius, and orientation. They demonstrated that the scale of the stimulus does not significantly impact radial deformation sensitivity. This suggests that the global shape, rather than the specific spatial frequency content, is the primary determinant of performance. As for the relationship between hyperacuity and contrast, it is well-established that Vernier acuity is strongly dependent on stimulus contrast at lower contrasts (McIlhagga & Pääkkönen, 2003). In our case, stimuli were presented at full contrast, at which hyperacuity thresholds tend to be independent of contrast (McIlhagga & Pääkkönen, 2003). Given that we link radial deformation sensitivity with hyperacuity in our discussion, it is reasonable to expect that contrast may also influence RF perception at lower contrasts. It would be an interesting avenue for future research to investigate how contrast affects the development of radial deformation sensitivity and whether this mirrors the contrast dependence of Vernier acuity.

Neurophysiological evidence also supports the role of global context in form processing within the ventral visual stream. Bushnell, Harding, Kosai, and Pasupathy, (2011) showed that V4 neurons exhibit context-dependent sensitivity to contour elements, with reduced responses to preferred elements when they are segmented from the coherent whole. Our laboratory's unpublished physiology work using RF patterns further supports this notion of spatial integration influencing neuronal coding. Our interpretation is that, although a local curvature mechanism like probability summation (Baldwin et al., 2016; Schmidtmann & Kingdom, 2017) may be sufficient under certain stimulus arrangements, substantial data indicate that global context influences perceptual judgements of RF patterns. Further investigation into the specific mechanisms is certainly warranted to understand what interplay of local and global cues enable the perception of this sort of intermediate shape.

Four-choice oddity and two-AFC task comparison

Our data are novel because they provide a characterization of global form sensitivity development using two psychophysical methods. In our comparison, we observed that both the oddity and discrimination tasks capture similar developmental trajectories with an approximately two times scaling difference in sensitivity between tasks. The difference in scaling between our datasets may reflect the inherent differences in decision variable mapping between a four-choice oddity and a 2-AFC discrimination task, given the lower number of alternatives in the 2-AFC. Prior literature shows that oddity tasks are learned faster and more accurately than their matching or identification counterparts, given the cognitive requirement of understanding the concept of "sameness" in matching tasks (Daniel, Wright, & Katz, 2016; Miller & Shettleworth, 2007). This is to say, oddity tasks do not require understanding the stimulus content. In the oddity task, animals can saccade toward a target by evaluating relative aspects between the stimuli and choosing the odd one out. The 2-AFC discrimination, however, requires a slightly different cognitive strategy in which animals may depend on observing the absolute values of the relevant stimulus dimension—or its identity—to choose between a circle versus radially deformed pattern (Bowers, 1976; Milton & Pothos, 2011). This is supported by findings suggesting that oddity discriminations activate the parietal cortex, while matching tasks are reliant on prefrontal cortex activation (Odgaard, Arieff, Kerr, & Laurienti, 2003; Mevorach, Humphreys, & Shalev, 2006). Practice, fatigue and/or attentional strategies may manifest differently between the two tasks and may potentially explain sensitivity differences. The four-choice oddity task proved beneficial for collecting thousands of trials in a shorter period of time at the earlier ages we tested. Jointly modeling the complementary 2-AFC and four-choice data sets allowed more reliable estimation of the developmental trajectory.

It is worth noting that we did notice a tendency for some animals to exhibit a bias toward one of the four possible target locations on the screen on the four-choice oddity task. The bias varied from animal to animal and each animal's bias shifted at different age points, which may be suggestive of shifting strategic approaches to the task requirements. Biases may evolve based on changes in reward expectations as the animals mature. However, the inclusion of catch trials, in which all stimuli were identical, allowed us to track these biases over time. Analysis of the catch trial performance revealed no consistent bias patterns across animals. Although individual animals showed biases shifting between different locations at different ages, these biases were distributed randomly rather than suggesting any systematic strategic approach. Furthermore, the shifting nature of the individual animal biases indicates they were unlikely to account fully for the clear developmental improvements on non-catch oddity trials. Thus, catch trial performance suggests that the observed developmental gains reflect improving perceptual abilities rather than simply emerging biases. Going forward, mapping trajectories of catch trial bias against oddity performance on a trial-by-trial basis could elucidate any potential strategic interplay and remains an open avenue for upcoming research.

Future directions

In this study, we showed that global form perception as measured with RF patterns is not fully mature in early infancy. This may reflect protracted development of visual analysis processes involved in the integration of shape signals across space. Object perception depends on a hierarchy of processing stages within the visual cortex (Van Essen, Anderson, & Felleman, 1992). A potential model of RF pattern perception has been proposed by Poirier and Wilson (2006). This model sums across oriented filters to extract contour information and implements triads of oriented center-surround filters tuned to different degrees of curvature to encode local curvature signals and identify points of maximum convex curvature (Poirier & Wilson, 2006). In the last processing stage, shape is represented as curvature signal strength as a function of orientation (polar angle) around the object's center, a computation associated with population codes in V4, which have been found to yield position invariant shape information (Pasupathy, 2006; Pasupathy & Connor, 2002). Human studies on visually evoked potentials have shown neural signatures of global form perception and hyperacuity exhibit a protracted maturational timecourse (Norcia et al., 2005; Pei et al., 2007; Pei et al., 2009; Palomares et al., 2010; Candy, Skoczenski, & Norcia, 2001; Skoczenski & Norcia, 2002). Whether postnatal maturation of V4 underlies the developmental trajectory reported here remains an open question and is the subject of an upcoming study from our laboratory.

Conclusions

We found that infant macaques could report global form early in development, although this ability continues to develop well into adolescence. We find evidence of lower sensitivity of global form mechanisms to the lowest RF. This likely reflects the visual system's prioritization of high RF processing critical for visual acuity and fine detail perception during development. We conclude that the neural mechanisms that integrate curvature features across space and decode increasingly smaller deviations between circles and RF patterns are not fully mature by the first year of age.

Keywords: global form perception, visual development, hyperacuity, non-human primates, psychophysics

Acknowledgments

The authors thank the NYU CNS Visual Neuroscience Lab, particularly Jessica Fletcher, Tiffany Tang, Kahlia Gronthos, Karen Fudge, and Solmaz Shariat Torbaghan, for training and testing our subjects. Thanks to the NYU Office of Veterinary Resources, our subjects, and the taxpaying public for funding NIH T32-MH019524 to L.K., R01-EY031446 to N.J.M., R01-EY024914 to J.A.M., F31-EY031592 to C.L.R.D., and F31-EY031249 to G.M.L.

Commercial relationships: none.
Corresponding author: C.L. Rodríguez Deliz.
Email: crd373@nyu.edu.
Address: Center for Neural Science, New York University, NY, USA.

[1]Present address: Department of Biological Structure, University of Washington, Seattle, WA, USA.

References

Atkinson, J., & Braddick, O. (2020). Visual development. In *Handbook of clinical neurology,* (vol. *173*, pp. 121–142). Elsevier.

Badcock, D., & Clifford, C. (2006). The inputs to global form detection. In *Seeing spatial form,* (pp. 43–56). Oxford University Press.

Badcock, D. R., Clifford, C. W., & Khuu, S. K. (2005). Interactions between luminance and contrast

signals in global form detection. *Vision Research, 45*(7), 881–889.

Baldwin, A. S., Schmidtmann, G., Kingdom, F. A., & Hess, R. F. (2016). Rejecting probability summation for radial frequency patterns, not so quick! *Vision Research, 122*, 124–134.

Bell, J., Badcock, D. R., Wilson, H., & Wilkinson, F. (2007). Detection of shape in radial frequency contours: Independence of local and global form information. *Vision Research, 47*(11), 1518–1522.

Birch, E. E., Swanson, W. H., & Wang, Y.-Z. (2000). Infant hyperacuity for radial deformation. *Investigative Ophthalmology & Visual Science, 41*(11), 3410–3414.

Blakemore, C., & Vital-Durand, F. (1986). Organization and post-natal development of the monkey's lateral geniculate nucleus. *Journal of Physiology, 380*(1), 453–491.

Boothe, R. G., Dobson, V., & Teller, D. Y. (1985). Postnatal development of vision in human and nonhuman primates. *Annual Review of Neuroscience, 8*(1), 495–545.

Boothe, R. G., Kiorpes, L., Williams, R. A., & Teller, D. Y. (1988). Operant measurements of contrast sensitivity in infant macaque monkeys during normal development. *Vision Research, 28*(3), 387–396.

Bowers, N. P. (1976). Rule learning and transfer in oddity and discrimination problems. *Child Development, 47*(4), 1130–1137.

Braddick, O., & Atkinson, J. (2007). Development of brain mechanisms for visual global processing and object segmentation. *Progress in Brain Research, 164*, 151–168.

Braddick, O., & Atkinson, J. (2011). Development of human visual function. *Vision Research, 51*(13), 1588–1609.

Braddick, O., Atkinson, J., & Wattam-Bell, J. (2003). Normal and anomalous development of visual motion processing: Motion coherence and 'dorsal-stream vulnerability'. *Neuropsychologia, 41*(13), 1769–1784.

Brown, A. M. (1997). Vernier acuity in human infants: rapid emergence shown in a longitudinal study. *Optometry and Vision Science, 74*(9), 732–740.

Bushnell, B. N., Harding, P. J., Kosai, Y., & Pasupathy, A. (2011). Partial occlusion modulates contour-based shape encoding in primate area v4. *Journal of Neuroscience, 31*(11), 4012–4024.

Candy, T. R., Skoczenski, A. M., & Norcia, A. M. (2001). Normalization models applied to orientation masking in the human infant. *Journal of Neuroscience, 21*(12), 4530–4541.

Carkeet, A., Levi, D. M., & Manny, R. E. (1997). Development of vernier acuity in childhood. *Optometry and Vision Science, 74*(9), 741–750.

Chino, Y. M., Smith, E. L., III, Hatta, S., & Cheng, H. (1997). Postnatal development of binocular disparity sensitivity in neurons of the primate visual cortex. *Journal of Neuroscience, 17*(1), 296–307.

Curran, W., Braddick, O., Atkinson, J., & Wattam-Bell, J. (2000). Form coherence perception in infancy. *Paper presented at the International Conference on Infant Studies,* Brighton, UK.

Daniel, T. A., Wright, A. A., & Katz, J. S. (2016). The oddity preference effect and the concept of difference in pigeons. *Learning & Behavior, 44*, 320–328.

Danka Mohammed, C. P., & Khalil, R. (2020). Postnatal development of visual cortical function in the mammalian brain. *Frontiers in Systems Neuroscience, 14*, 29.

Daw, N. W. (2006). *Visual development* (Vol. *14*). Springer.

El-Shamayleh, Y., Movshon, J. A., & Kiorpes, L. (2010). Development of sensitivity to visual texture modulation in macaque monkeys. *Journal of Vision, 10*(11), 11–11.

Fantz, R. L. (1963). Pattern vision in newborn infants. *Science, 140*(3564), 296–297.

Fantz, R. L. (1964). Visual experience in infants: Decreased attention to familiar patterns relative to novel ones. *Science, 146*(3644), 668–670.

Farroni, T., Valenza, E., Simion, F., & Umilta, C. (2000). Configural processing at birth: Evidence for perceptual organisation. *Perception, 29*(3), 355–372.

Gerhardstein, P., Kovacs, I., Ditre, J., & Feher, A. (2004). Detection of contour continuity and closure in three-month-olds. *Vision Research, 44*(26), 2981–2988.

Glass, L. (1969). Moire effect from random dots. *Nature, 223*(5206), 578–580.

Glass, L., & Perez, R. (1973). Perception of random dot interference patterns. *Nature, 246*(5432), 360–362.

Gunn, A., Cory, E., Atkinson, J., Braddick, O., Wattam-Bell, J., Guzzetta, A., . . . Cioni, G. (2002). Dorsal and ventral stream sensitivity in normal development and hemiplegia. *Neuroreport, 13*(6), 843–847.

Hacker, M. J., & Ratcliff, R. (1979). A revised table of d' for M-alternative forced choice. *Attention, Perception, & Psychophysics, 15*, 168–170.

Hadad, B.-S., Maurer, D., & Lewis, T. L. (2010). The development of contour interpolation: Evidence from subjective contours. *Journal of Experimental Child Psychology, 106*(2–3), 163–176.

Hershenson, M. (1964). Visual discrimination in the human newborn. *Journal of Comparative and Physiological Psychology, 58*(2), 270.

Hess, R. F., Achtman, R. L., & Wang, Y.-Z. (2001). Detection of contrast-defined shape. *JOSA A, 18*(9), 2220–2227.

Hess, R. F., Wang, Y.-Z., & Dakin, S. C. (1999). Are judgements of circularity local or global? *Vision Research, 39*(26), 4354–4360.

Humphrey, G. K., & Humphrey, D. E. (1989). The role of structure in infant visual pattern perception. *Canadian Journal of Psychology/Revue Canadienne de Psychologie, 43*(2), 165.

Humphrey, G. K., Humphrey, D. E., Muir, D. W., & Dodwell, P. C. (1986). Pattern perception in infants: Effects of structure and transformation. *Journal of Experimental Child Psychology, 41*(1), 128–148.

Humphrey, G. K., Muir, D. W., Dodwell, P. C., & Humphrey, D. E. (1988). The perception of structure in vector patterns by 4-month-old infants. *Canadian Journal of Psychology/Revue Canadienne de Psychologie, 42*(1), 35.

Jeffrey, B. G., Wang, Y.-Z., & Birch, E. E. (2002). Circular contour frequency in shape discrimination. *Vision Research, 42*(25), 2773–2779.

Johnson, S. P. (2011). Development of visual perception. *Wiley Interdisciplinary Reviews: Cognitive Science, 2*(5), 515–528.

Kaplan, H. L., Macmillan, N. A., & Creelman, C. D. (1978). Tables of d for variable-standard discrimination paradigms. *Behavior Research Methods & Instrumentation, 10*, 796–813.

Kimchi, R. (1992). Primacy of wholistic processing and global/local paradigm: A critical review. *Psychological Bulletin, 112*(1), 24.

Kimchi, R., Hadad, B., Behrmann, M., & Palmer, S. E. (2005). Microgenesis and ontogenesis of perceptual organization: Evidence from global and local processing of hierarchical patterns. *Psychological Science, 16*(4), 282–290.

Kiorpes, L. (1992). Development of vernier acuity and grating acuity in normally reared monkeys. *Visual Neuroscience, 9*(3-4), 243–251.

Kiorpes, L. (2015). Visual development in primates: Neural mechanisms and critical periods. *Developmental Neurobiology, 75*(10), 1080–1090.

Kiorpes, L., & Bassin, S. A. (2003). Development of contour integration in macaque monkeys. *Visual Neuroscience, 20*(5), 567–575.

Kiorpes, L., & Kiper, D. C. (1996). Development of contrast sensitivity across the visual field in macaque monkeys (Macaca nemestrina). *Vision Research, 36*(2), 239–247.

Kiorpes, L., Kiper, D. C., & Movshon, J. A. (1993). Contrast sensitivity and vernier acuity in amblyopic monkeys. *Vision Research, 33*(16), 2301–2311.

Kiorpes, L., & Movshon, J. (2014). Neural limitations on visual development in primates: Beyond striate cortex. In *The visual neurosciences,* 2nd edition. MIT Press.

Kiorpes, L., & Movshon, J. A. (1989). Differential development of two visual functions in primates. *Proceedings of the National Academy of Sciences of the United States of America, 86*(22), 8998–9001.

Kiorpes, L., & Movshon, J. A. (2003). Differential development of form and motion perception in monkeys. *Journal of Vision, 3*(9), 204–204.

Kiorpes, L., & Movshon, J. A. (2004). Neural limitations on visual development in primates. *Visual Neurosciences, 1*, 159–173.

Kiorpes, L., Price, T., Hall-Haro, C., & Movshon, J. A. (2012). Development of sensitivity to global form and motion in macaque monkeys (Macaca nemestrina). *Vision Research, 63*, 34–42.

Kovacs, I. (1996). Gestalten of today: Early processing of visual contours and surfaces. *Behavioural Brain Research, 82*(1), 1–11.

Kovacs, I., Kozma, P., Feher, A., & Benedek, G. (1999). Late maturation of visual spatial integration in humans. *Proceedings of the National Academy of Sciences of the United State of America, 96*(21), 12204–12209.

Kozma, P., & Kiorpes, L. (2003). Contour integration in amblyopic monkeys. *Visual Neuroscience, 20*(5), 577–588.

Lee, G. M., Rodríguez-Deliz, C., Bushnell, B. N., Majaj, N. J., Movshon, J. A., & Kiorpes, L. (2024). Developmentally stable representations of naturalistic image structure in macaque visual cortex. *bioRxiv,* 2024–02.

Lewis, T. L., Ellemberg, D., Maurer, D., Dirks, M., Wilkinson, F., & Wilson, H. R. (2004). A window on the normal development of sensitivity to global form in glass patterns. *Perception, 33*(4), 409–418.

Loffler, G. (2008). Perception of contours and shapes: Low and intermediate stage mechanisms. *Vision Research, 48*(20), 2106–2127.

Loffler, G., Wilson, H. R., & Wilkinson, F. (2003). Local and global contributions to shape discrimination. *Vision Research, 43*(5), 519–530.

Manny, R. E., & Klein, S. A. (1984). The development of vernier acuity in infants. *Current Eye Research, 3*(3), 453–462.

McIlhagga, W., & Pääkkönen, A. (2003). Effects of contrast and length on vernier acuity explained with noisy templates. *Vision Research, 43*(6), 707–716.

Mevorach, C., Humphreys, G. W., & Shalev, L. (2006). Odd object out: Evidence for an oddity advantage in object based neglect. *Neuropsychologia, 44*(7), 1105–1117.

Miller, R. R., & Shettleworth, S. J. (2007). Oddity and prototype learning in humans compared to learning in pigeons. *Learning Behavior, 35*(2), 80–96.

Milton, F., & Pothos, E. M. (2011). The oddity of 'oddity': A conceptual re-evaluation and a unified theory. *Cognition, 121*(3), 412–432.

Nayar, K., Franchak, J., Adolph, K., & Kiorpes, L. (2015). From local to global processing: The development of illusory contour perception. *Journal of Experimental Child Psychology, 131*, 38–55.

Norcia, A. M., Manny, R. E., & Wesemann, W. (1988). Vernier acuity measured using the sweep VEP. In *Noninvasive assessment of the visual system Technical Digest Series (Optica Publishing Group, 1988), paper ThA4ThA4*.

Norcia, A. M., Pei, F., Bonneh, Y., Hou, C., Sampath, V., & Pettet, M. W. (2005). Development of sensitivity to texture and contour information in the human infant. *Journal of Cognitive Neuroscience, 17*(4), 569–579.

Odgaard, E. C., Arieff, A. J., Kerr, D. L., & Laurienti, P. J. (2003). FMRI activation in the middle frontal gyrus as an indicator of hemispheric dominance for the oddity task. *Laterality: Asymmetries of Body, Brain and Cognition, 8*(2), 137–147.

Palomares, M., Pettet, M., Vildavski, V., Hou, C., & Norcia, A. (2010). Connecting the dots: How local structure affects global integration in infants. *Journal of Cognitive Neuroscience, 22*(7), 1557–1569.

Palomares, M., & Shannon, M. T. (2013). Global dot integration in typically developing children and in Williams syndrome. *Brain and Cognition, 83*(3), 262–270.

Pasupathy, A. (2006). Neural basis of shape representation in the primate brain. *Progress in Brain Research, 154*, 293–313.

Pasupathy, A., & Connor, C. E. (2002). Population coding of shape in area v4. *Nature Neuroscience, 5*(12), 1332–1338.

Pei, F., Baldassi, S., Procida, G., Igliozzi, R., Tancredi, R., Muratori, F., ... Cioni, G. (2009). Neural correlates of texture and contour integration in children with autism spectrum disorders. *Vision Research, 49*(16), 2140–2150.

Pei, F., Pettet, M. W., & Norcia, A. M. (2007). Sensitivity and configuration-specificity of orientation-defined texture processing in infants and adults. *Vision Research, 47*(3), 338–348.

Poirier, F. J., & Wilson, H. R. (2006). A biologically plausible model of human radial frequency perception. *Vision Research, 46*(15), 2443–2455.

Quinn, P. C. (2000). Perceptual reference points for form and orientation in young infants: Anchors or magnets? *Perception & Psychophysics, 62*(8), 1625–1633.

Scherf, K. S., Behrmann, M., Kimchi, R., & Luna, B. (2009). Emergence of global shape processing continues through adolescence. *Child Development, 80*(1), 162–177.

Schmidtmann, G., & Kingdom, F. A. (2017). Nothing more than a pair of curvatures: A common mechanism for the detection of both radial and non-radial frequency patterns. *Vision Research, 134*, 18–25.

Schwartz, M., Day, R. H., & Cohen, L. B. (1979). Visual shape perception in early infancy. *Monographs of the Society for Research in Child Development, 44*(7), 1–63.

Shimojo, S., Birch, E. E., Gwiazda, J., & Held, R. (1984). Development of vernier acuity in infants. *Vision Research, 24*(7), 721–728.

Shimojo, S., & Held, R. (1987). Vernier acuity is less than grating acuity in 2-and 3-month-olds. *Vision Research, 27*(1), 77–86.

Skoczenski, A. M., & Norcia, A. M. (2002). Late maturation of visual hyperacuity. *Psychological Science, 13*(6), 537–541.

Smith, L. B. (2009). From fragments to geometric shape: Changes in visual object recognition between 18 and 24 months. *Current Directions in Psychological Science, 18*(5), 290–294.

Subramanian, V., Morale, S. E., Wang, Y.-Z., & Birch, E. E. (2012). Abnormal radial deformation hyperacuity in children with strabismic amblyopia. *Investigative Ophthalmology & Visual Science, 53*(7), 3303–3308.

Teller, D. Y. (1981). The development of visual acuity in human and monkey infants. *Trends in Neurosciences, 4*, 21–24.

Teller, D. Y. (1997). First glances: The vision of infants. the Friedenwald Lecture. *Investigative Ophthalmology & Visual Science, 38*(11), 2183–2203.

Teller, D. Y., & Movshon, J. A. (1986). Visual development. *Vision Research, 26*(9), 1483–1506.

Van Essen, D. C., Anderson, C. H., & Felleman, D. J. (1992). Information processing in the primate visual system: An integrated systems perspective. *Science, 255*(5043), 419–423.

Wang, Y.-Z., & Hess, R. F. (2005). Contributions of local orientation and position features to shape integration. *Vision Research, 45*(11), 1375–1383.

Wang, Y.-Z., Morale, S. E., Cousins, R., & Birch, E. E. (2009). The course of development of global hyperacuity over lifespan. *Optometry and Vision Science, 86*(6), 695.

Wattam-Bell, J., Birtles, D., Nystrom, P., Von Hofsten, C., Rosander, K., Anker, S., … Braddick, O. (2010). Reorganization of global form and motion processing during human visual development. *Current Biology, 20*(5), 411–415.

Westheimer, G. (2010). Visual acuity and hyperacuity. *Handbook of Optics, 3*, 4–1.

Wichmann, F. A., & Hill, N. J. (2001a). The psychometric function: I. Fitting, sampling, and goodness of fit. *Perception & Psychophysics, 63*(8), 1293–1313.

Wichmann, F. A., & Hill, N. J. (2001b). The psychometric function: II. Bootstrap-based confidence intervals and sampling. *Perception & Psychophysics, 63*, 1314–1329.

Wilkinson, F., Wilson, H. R., & Habak, C. (1998). Detection and recognition of radial frequency patterns. *Vision Research, 38*(22), 3555–3568.

Wilson, H. R., Wilkinson, F., & Asaad, W. (1997). Concentric orientation summation in human form vision. *Vision Research, 37*(17), 2325–2330.

Zanker, J., Mohn, G., Weber, U., Zeitler-Driess, K., & Fahle, M. (1992). The development of vernier acuity in human infants. *Vision Research, 32*(8), 1557–1564.